forests

MDPI

Article

Short-Term Variation in Soil Organo-Mineral Associations in Alpine Forest–Shrub Transitional Zone on the Eastern Tibetan Plateau

Mingxuan Che †, Yinying Shuai †, Jie Liu, Yuting Song, Ruifa Wang, Hongyi Yuan, Mingxue Liu and Gang Xu *

College of Life Sciences and Agri-Forestry, Southwest University of Science and Technology, Mianyang 621010, China; cmxstbc@163.com (M.C.); syy1232025@163.com (Yinying Shuai)
* Correspondence: xugang@swust.edu.cn
† These authors contributed equally to this work.

Abstract

Soil organo-mineral associations (OMAs) play key roles in soil organic carbon (SOC) long-term persistence. However, OMAs may be sensitive to biotic inputs, such as litter and root exudates, as well as to soil physicochemical properties, including pH and cation concentrations. In alpine forest–shrub transitional zones, pronounced seasonal changes in environmental conditions may drive biogeochemical processes that alter OMAs over short timescales. Nevertheless, the short-term dynamics of OMAs remain poorly understood. Here, we combined field sampling across three seasons with an in situ vegetation-removal incubation to examine seasonal and post-winter changes in extractable carbon associated with different Al- and Fe-bearing fractions in an alpine forest–shrub transitional zone on the eastern Tibetan Plateau. Sodium pyrophosphate (PP), hydroxylamine hydrochloride (HH), and dithionite-HCl (DH) extractions were used to operationally quantify organo-metal complexes, SOC associated with short-range-order (SRO) mineral phases, and SOC associated with crystalline mineral phases, respectively. In the vegetation-removal incubation, DH-extractable fraction (C_{DH}) exhibited a significant, albeit small, decrease (approximately 7.7%), which coincided with an increase in soil pH. Under natural seasonal conditions, the highest concentration of HH-extractable carbon (C_{HH}) occurred in October, consistent with the seasonal pattern of SOC, whereas C_{DH} and PP-extractable carbon (C_{PP}) showed little variation among seasons. Extracted C-to-metal molar ratio (C/M; C relative to Al + Fe) and the proportions of extracted C to SOC also varied among sampling periods. The results demonstrate short-term variation in extractable OMA-associated C fractions and their ratios to SOC. These findings highlight the short-term variability of operationally defined OMA-associated carbon pools in alpine soils and improve our understanding of SOC cycling in alpine ecosystems.

Keywords: soil organic carbon; organo-mineral associations; in situ incubation; short-term dynamics; forest–shrub transitional zone

Check for updates

Academic Editors: Shuai Wang and Yang Wang

Received: 21 October 2026
Revised: 11 November 2026
Accepted: 17 November 2026
Published: 19 November 2026

Copyright: © 2026 by the authors. Licensee MDPI, Basel, Switzerland. This article is an open access article distributed under the terms and conditions of the Creative Commons Attribution (CC BY) license.

1. Introduction

The soil organic carbon (SOC) pool stores approximately 1580 Gt of organic carbon, which is twice the size of the atmospheric carbon pool and three times the size of the vegetation biomass carbon pool [1,2]. Depending on the balance between carbon inputs and losses, soils may act as either a carbon source, releasing greenhouse gases through SOC decomposition, or a carbon sink, sequestering carbon from the atmosphere [3,4].

This potential for soils to act as either a source or a sink highlights the importance of SOC persistence, commonly considered in terms of its resistance to decomposition or mineralization [5,6].

Interactions between SOC and reactive minerals are important mechanisms governing long-term C persistence [7–10]. Aluminum (Al) and iron (Fe), the third and fourth most abundant elements in the Earth's crust, play key roles in C accumulation and stability due to their highly reactive surface properties and prevalence. These metals and minerals can strongly bind with organic matter through sorption and coprecipitation and thereby form organo-mineral associations (OMAs) [10,11]. The formation of OMAs is assumed to limit microbial and enzymatic access, thereby allowing the organic carbon to persist [9,10]. Moreover, short-range-order (SRO) minerals and Fe oxides can also promote aggregation, which further indirectly enhances organic carbon stability [12,13]. This assumption was supported by both laboratory and field studies, which found that the formation of OMAs reduces organic carbon mineralization [14–16] and that OMAs exhibit older average ages than other fractions based on radiocarbon (^{14}C) analyses [9,17,18]. However, recent studies challenged the role of OMAs in long-term SOC stability, as some factors (e.g., root and microbial exudates, soil pH, oxygen supply, and C substrate addition) may liberate organic matter protected by minerals and thereby enhance its decomposition [12,19–21].

Plant litter and root-derived C are important for SOC accumulation, contributing up to 50%–70% of total soil C stocks [22]. Exudates produced by root (e.g., oxalic acid) and root-associated microbes would accelerate primary mineral weathering, creating secondary crystalline and poorly crystalline Fe and Al phases that act as templates for the formation of OMAs [23–25]. Conversely, these exudates can also dissolve secondary mineral phases, liberate C previously protected by these minerals, and make it more susceptible to microbial conversion to CO_2 [20,26]. Although the consequence of root-driven C balance is inconsistent, the role of root activity in OMA disturbance is emphasized. As root activity is seasonally dynamic and leads to a seasonal distribution of different crystallinity minerals [27], the composition and amounts of OMAs may also be seasonally dynamic. Moreover, organic carbon associated with minerals of different crystalline phases may exhibit different C turnover patterns [28]. Thus, OMA stabilities may be further influenced by the dynamics of mineral crystallinity on a short time scale. However, the seasonal dynamics of OMAs are less studied.

In addition to vegetation-related effects, winter conditions in high-altitude environments can alter soil physical and chemical properties and may thereby affect OMAs. For example, soil freeze–thaw (FT) events are a common phenomenon in high-latitude and high-elevation ecosystems [29]. As a non-biological stress, the FT process can substantially alter soil biogeochemical processes, thereby affecting C cycling [30,31]. The FT process is known to destroy microorganisms and root cells, increasing the concentration of labile organic matter and other nutrient elements in the soil solution [32,33]. In addition, the FT process can also break soil aggregates induced by ice expansion and contraction processes, exposing organic matter previously protected in aggregates, thereby increasing microbial spatial accessibility [33–35]. Moreover, soil physicochemical conditions would also be significantly influenced by the FT process. Studies suggest that soil pH, exchangeable and colloidal Al, Fe, and Ca elements, soil particle and mineral composition, hydrology, and oxygen conditions, which closely correlate with OMAs, are also strongly affected by the FT process [36,37]. However, how changes in organic matter and sorbent availability, including Al and Fe cations and minerals, as well as associated soil conditions, affect OMAs remains unclear.

The Tibetan Plateau ranks among the most rapidly warming ecosystems in the world and is a highly sensitive model area for studying climate change impacts [38]. The forest–

shrub transitional zone is particularly sensitive to environmental changes, due to its extremely high-altitude conditions [39,40]. Previous studies of treelines and shrublines on the Tibetan Plateau have focused primarily on aboveground vegetation responses to climate change, whereas belowground soil dynamics remain less well understood [38,41]. A clear understanding of SOC dynamics in alpine soil is necessary due to high C concentration and potential feedback responses to climate change [42,43]. Although Al- and Fe-associated organic matter has been studied in a range of ecosystems, short-term variation in operationally defined carbon fractions associated with different Al- and Fe-bearing phases remains insufficiently characterized in alpine forest–shrub transitional zones. In particular, it is unclear whether these fractions differ among growing season, autumn, and post-winter sampling periods, and whether changes in extractable carbon during a vegetation-removal incubation are accompanied by changes in extractable C-to-metal ratios. Selective dissolution provides operationally defined fractions and does not directly measure carbon persistence or turnover time. Accordingly, changes in these fractions are interpreted as changes in extractable pools rather than as direct evidence of stabilization or destabilization.

This study addressed three questions: (1) Do PP-, HH-, and DH-extractable carbon concentrations and their proportions relative to SOC differ among seasonal sampling periods? (2) Do these measures differ between the two sampling times of a vegetation- and root-removal incubation spanning the winter period? (3) Are changes in extractable carbon accompanied by changes in extractable C-to-metal ratios? We hypothesized that extractable carbon fractions would differ among sampling periods and soil depths, and that at least some extractable fractions would change during the winter-spanning incubation.

2. Materials and Methods

2.1. Study Site and Soil Sampling

This study was conducted in the western Zheduo Mountain region (30°00′–30°08′ N, 101°44′–101°51′ E), Ganzi Tibetan Autonomous Prefecture, Sichuan Province, China, located on the eastern edge of the Qinghai–Tibet plateau. Study area is the transitional zone of forest and shrub meadow. The altitudes range from 3 803 m to 3910 m. Vegetation was dominated by a mixture of small trees and shrubs. The main vegetation species are *Sabina squamata* (Buch.-Ham. ex D. Don) Antoine, *Picea asperata* Mast., *Abies fabri* (Mast.) Craib, *Berberis amurensis* Rupr., *Rhododendron telmateium* Balf. f. et W. W. Sm., and *Potentilla fruticosa* L. The area experiences an intermediate climate, ranging between a sub-frigid monsoon and plateau continental climates, with abundant sunshine, cold winters, and cool summers [44]. The mean annual temperature is 7.1 °C, with a mean temperature of 12.7 °C in August (the warmest month) and −5.8 °C in January (the coldest month). The mean annual precipitation is 827.2 mm, and the mean annual sunshine hours are 1715 h [44]. The growing season is commonly from early May to early October. The soil was classified as dark brown earth based on the Chinese Soil Taxonomy (CST), with a silty loam texture and 25.6% sand, 58.0% silt, and 16.4% clay.

Soil samples were collected in August 2017 (summer, growing season), October 2017 (first observed snowfall we defined it as the beginning of winter, the dormant season), and May 2018 (snowfall totally melted, we defined it as the beginning of spring, the recovery season) from five sites located on the western slope of Zheduo Mountain. We selected five typical forest–shrub transitional zone sites on the mountain. In each site, three soil plots (5 × 5 m, at least 200 m apart) were established. In each plot, five subsamples were collected from each of two depths (0–20 and 20–40 cm) and composited by depth. Thus, each sampling period comprised 15 plot-level composite samples per depth. The same plots were sampled on all three dates. Soil samples were gently crumbled and sieved manually in the field to an approximate particle size of <2 mm to remove aboveground biomass, roots,

and stones. Following collection, the samples designated for DOC and MBC analyses were transported to the laboratory in an insulated cooler and stored at 4 °C until analysis. The remaining samples were air-dried at room temperature for chemical analyses.

2.2. Soil In Situ Incubation and Sampling

We established a soil-cylinder incubation at the same sites to examine changes in soil properties and operationally defined extractable C fractions across the winter period under vegetation and root removal. To reduce continuing inputs from vegetation and roots, soil was manually cleared of visible roots and aboveground plant material before being packed into PVC cylinders (40 cm in length, 10 cm in diameter). According to the mean bulk densities of fresh soil at the study sites, soil from the 0–20 cm layer was packed to a bulk density of 1.2 g cm^{-3}, whereas soil from the 20–40 cm layer was packed to 1.4 g cm^{-3}. The two soil layers were packed into each PVC cylinder in their original vertical order and kept separate. Thus, each cylinder contained a 0–20 cm layer overlying a 20–40 cm layer. In August 2017, two cylinders were installed in each plot and assigned to the October 2017 and May 2018 sampling dates, respectively. Upon retrieval, each cylinder yielded two depth-specific soil samples. Therefore, 15 observations were obtained for each soil depth at each sampling time (five sites × three plots). The cylinder ends were covered with nylon mesh and secured with elastic bands to limit animal access and litter entry while water and gas exchange remained possible. Because some studies showed that low-molecular-weight compounds were produced mainly in autumn from the leaching of fresh litter, these compounds interact easily with soil minerals [20,26,45]. However, comparisons between the field samples and the cylinder samples were intended only to provide a descriptive comparison between natural seasonal conditions and the vegetation- and root-removal incubation conditions. Because these conditions also differed in soil structure, pore conditions, microbial activity, and substrate availability, the comparison was not interpreted as an estimate of the isolated effects of vegetation removal, root exudates, or litter inputs.

Cylinders were retrieved in October 2017 (pre-winter) and May 2018 (post-winter, after snowmelt), with 15 cylinders (5 sites × 3 plots) collected at each time point. These samples were transported to the laboratory within 24 h and processed following the same procedure illustrated above. It should be noted that this treatment was intended to reduce continuing root and litter inputs; however, it may also have altered soil structure and pore conditions and affected microbial activity and substrate availability. Thus, differences between the field samples and the cylinders cannot be attributed solely to root exudates or vegetation inputs.

2.3. Analyses of Basic Soil Properties

SOC was determined via dichromate oxidation. Soil pH was measured using a 1 M KCl suspension (1:5 w/v) with a glass electrode. The exchangeable cations (K, Na, Al, Fe, Mg, Mn, and Ca) were extracted with 1 M NH_4NO_3 and measured using inductively coupled plasma optical emission spectrometry (ICP-OES; Thermo Fisher Scientific, Waltham, MA, USA) [46]. The concentrations of the seven soil exchangeable cations were calculated on an equivalent basis and were expressed as mmol (+) kg^{-1} soil. Soil effective cation exchange capacity (ECEC) was calculated as the sum of the seven exchangeable cations [47]. Soil MBC was measured by the fumigation-extraction method, while the DOC was measured by the extracted C of the unfumigated samples using a multi N/C 2100 analyzer (Analytik Jena AG, Jena, Germany). [48].

2.4. Selective Dissolution Extractions

We applied the selective dissolution method to operationally estimate C in extracts associated with different Al- and Fe-bearing fractions using three C-free extractions. They are not perfectly selective for individual mineral phases, and the extracted C concentrations, C/SOC proportions, and C/(Al + Fe) ratios do not directly measure carbon persistence, turnover time, or stabilization. Accordingly, we refer to these measurements as PP-, HH-, and DH-extractable C and as extractable C-to-metal ratios. Interpretations concerning mineral association or possible carbon–mineral interactions are presented as cautious inferences rather than direct measurements of process or stability. Although these methods are not as selective in some cases, they provide a useful and broadly recognized semiquantitative assessment [49]. The studies that suggested that extractable metal contents often show significant correlation with soil C storage and turnover times also highlight the importance of this method [18,24,49–51].

Briefly, the Dithionite-HCl (DH; 57.4 mM Na dithionite at pH 3, followed by a 1 N HCl rinse), was used to mainly extract SOC associated with the pedogenic Fe phases (i.e., solid Fe oxides, hydroxides, and oxyhydroxides). It could also extract some of the non-crystalline phases and organo-metal complexes [11]. The acidified hydroxylamine (HH; 0.25 M NH_2OH·0.25 N HCl at pH 3, in the dark) was used to extract SOC associated with SRO and other non-crystalline phases, with minor dissolution of crystalline oxides. Na-pyrophosphate (PP; 0.1 M Na pyrophosphate at pH 10) was used to primarily extract organo-metal complexes, although it may also dissolve some (<10%) non-crystalline SRO minerals [49].

In each case, 0.5 g soil was mixed with 30 mL of each extractant in a 50 mL centrifuge tube. Soil samples were shaken for 16 h and then centrifuged for 120 min at 5300× *g*. The supernatant was subsequently decanted and syringe-filtered through a 0.2 µm nylon membrane filter (Whatman GD/X syringe filter, 25 mm diameter; Cytiva, Marlborough, MA, USA) into 50 mL sample tubes. For DH extraction, supernatants from Na dithionite and HCl were combined and analysed for C and metal concentrations. Extractant controls (i.e., extractant without soil samples) were also analysed for C and metal concentrations to eliminate extractant error. The detailed interpretations of extracted materials are included in the Supplementary Materials.

2.5. Statistical Analysis

Measurements are presented as means (standard errors). The plot-level composite sample was the experimental unit for field sampling; the five subsamples collected within each plot were pooled and therefore were not treated as independent replicates. For seasonal field data, sampling period, soil depth, and their interaction were treated as fixed effects. Site and plot nested within a site were considered grouping factors; repeated sampling of the same plot across periods was accounted for in the model. For the cylinder incubation, the cylinder was the sampling unit and the dependence of cylinders from the same plot and site was accounted for where supported by the sampling design. Model structure and the treatment of repeated observations were specified before testing fixed effects. Residual distributions and model assumptions were checked. Mixed-effect models were used to examine the effects of sampling period, soil depth, and interactions between these factors on soil parameters (i.e., SOC, DOC, MBC, pH, and ECEC) and organo-mineral associations (Fe, Al, and C concentrations and the molar ratio of C to metals in each stage). Correlation analyses were performed separately for Season and Incubation. Uncertainty was assessed using a site-stratified, plot-level cluster bootstrap to account for repeated measurements within plots. Regressions between extracted C and extracted Al + Fe were determined using a linear mixed-effects model. Post hoc comparisons were adjusted for multiple testing.

Statistical significance was assessed at $p < 0.05$. All data were analyzed using R version 4.5.2 (R Foundation for Statistical Computing, Vienna, Austria).

3. Results

3.1. Variations in Basic Soil Properties

The winter-spanning incubation significantly affected soil pH, DOC, and MBC (Table 1). Compared with the pre-winter sampling, soil pH increased significantly by 0.2 units after winter, whereas soil effective cation exchange capacity (ECEC) increased by 19.2%; however, the difference was not significant. Soil organic carbon (SOC) showed a slight, nonsignificant decrease after winter, while DOC and MBC were significantly higher in the post-winter samples than in the pre-winter samples.

Table 1. Basic soil properties at different sampling stages.

Soil Properties	Soil Depth	Season			Incubation	
		August	October	May	Pre-Winter	Post-Winter
SOC ($g\ kg^{-1}$)	0–20 cm	57.6 (8.7) Aa	67.3 (9.7) Ba	55.7 (10.3) Aa	52.2 (10.0) Aa	51.4 (8.6) Aa
	20–40 cm	35.8 (9.3) Ab	38.9 (9.2) Bb	30.2 (13.1) Ab	32.8 (5.8) Ab	30.2 (6.0) Ab
DOC ($mg\ kg^{-1}$)	0–20 cm	172.9 (41.2) Aa	118.2 (37.4) Ba	154.4 (47.6) Ca	106.3 (25.9) Aa	142.3 (33.4) Ba
	20–40 cm	133.8 (57.0) Ab	72.6 (50.8) Bb	97.0 (42.7) Cb	79.0 (32.4) Ab	120.4 (43.4) Bb
MBC ($mg\ kg^{-1}$)	0–20 cm	438.8 (212.7) Aa	378.9 (174.3) Aa	683.6 (206.7) Ba	244.3 (104.3) Aa	557.0 (204.7) Ba
	20–40 cm	150.5 (88.2) Ab	171.9 (77.5) Ab	226.3 (100.5) Bb	145.9 (89.4) Ab	274.5 (116.0) Bb
pH	0–20 cm	4.3 (0.3) Aa	4.3 (0.2) Aa	4.3 (0.2) Aa	4.2 (0.1) Aa	4.4 (0.1) Ba
	20–40 cm	4.5 (0.2) Ab	4.5 (0.2) Ab	4.5 (0.2) Ab	4.4 (0.1) Ab	4.6 (0.1) Bb
ECEC ($mmol\ kg^{-1}$)	0–20 cm	20.5 (7.8) Aa	21.6 (12.3) Aa	21.6 (10.9) Aa	21.8 (10.5) Aa	26.3 (10.2) Aa
	20–40 cm	10.5 (6.7) Ab	8.4 (2.9) Ab	11.0 (7.6) Ab	12.8 (3.5) Ab	14.5 (3.8) Ab

Note: SOC, DOC, MBC, and ECEC mean soil organic carbon, dissolved organic carbon, microbial biomass carbon, and effective cation exchange capacity, respectively. Values are means ± SE. Within each panel, lowercase letters indicate significant differences between soil depths within a sampling period; uppercase letters indicate significant differences among sampling periods within the same soil depth ($p < 0.05$). For the incubation comparison, uppercase letters indicate differences between pre-winter and post-winter samples within the same soil depth. The statistical model and post hoc procedure are described in Section 2.5.

Significant seasonal differences were observed in SOC, DOC, and MBC (Table 1), whereas soil pH and ECEC did not differ significantly among sampling periods. SOC was significantly higher in October than in August and May. DOC was highest in August, followed by May and October. MBC was significantly higher in May than in August and October.

3.2. Variation in Al and Fe Mineral Fractions

Compared with the pre-winter samples, PP-extractable Al and Fe concentrations were significantly higher after winter (Figure 1). In contrast, HH-extractable Al and Fe showed slight decreases in the post-winter samples, although these changes were not significant. Across both the seasonal sampling and incubation datasets, Al_{DH} was significantly lower in the 0–20 cm layer than in the 20–40 cm layer, whereas Fe_{PP} and Fe_{HH} were significantly higher in the 0–20 cm layer than in the 20–40 cm layer.

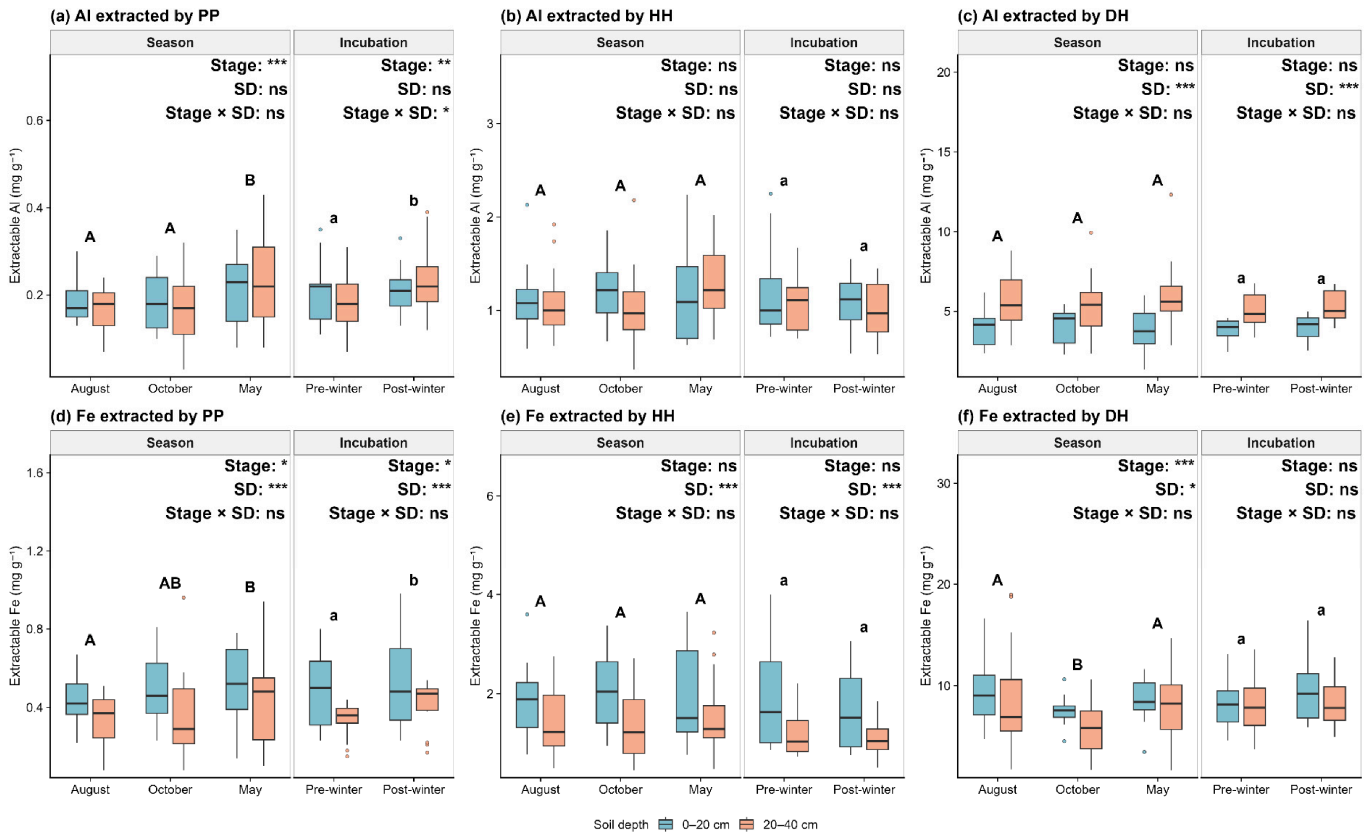


Figure 1. Extractable Al (**a**–**c**) and Fe (**d**–**f**) concentrations across seasonal sampling periods (Season) and vegetation-removal incubation stages (Incubation) at different soil depths (SDs). Soil samples were extracted using sodium pyrophosphate (PP), acidified hydroxylamine (HH), and dithionite–HCl (DH). The effects of sampling period or incubation stage (Stage), soil depth (SD), and their interaction (Stage × SD) were assessed using linear mixed-effects models (LMMs). Different uppercase letters indicate significant differences among seasonal sampling periods (marginal means over depth), whereas different lowercase letters indicate significant differences between pre-winter and post-winter incubation stages (marginal means over depth). Significance levels are indicated as ns ($p \geq 0.05$), * ($p < 0.05$), ** ($p < 0.01$), and *** ($p < 0.001$).

Seasonal sampling significantly affected only Al_{PP}, Fe_{PP}, and Fe_{DH}; the other measured Al and Fe fractions did not differ significantly among seasons (Figure 1). Al_{PP} was significantly higher in May than in August and October, with the difference being particularly pronounced in the 20–40 cm layer. Fe_{DH} decreased from August to October and subsequently increased from October to May.

3.3. Variation of Mineral-Associated C Fractions

In the vegetation-removal incubation system, the C_{PP}, C_{HH}, and C_{DH} tended to slightly decrease in post-winter, although only C_{DH} showed a significant pre- to post-winter difference (Figure 2). Contrary to seasonal variations, the proportions of C_{PP}, C_{HH}, and C_{DH} to SOC were similar in post-winter treatment and not affected by winter-spanning. The proportions of C_{PP}, C_{HH}, and C_{DH} to SOC did not differ significantly between the pre- and post-winter sampling times. Within the incubation dataset, the C_{PP}/SOC was significantly higher in the 20–40 cm layer than in the 0–20 cm layer. In contrast, within the seasonal dataset, C_{DH}/SOC was significantly higher at 20–40 cm than at 0–20 cm, whereas this depth difference was not significant in the incubation dataset.

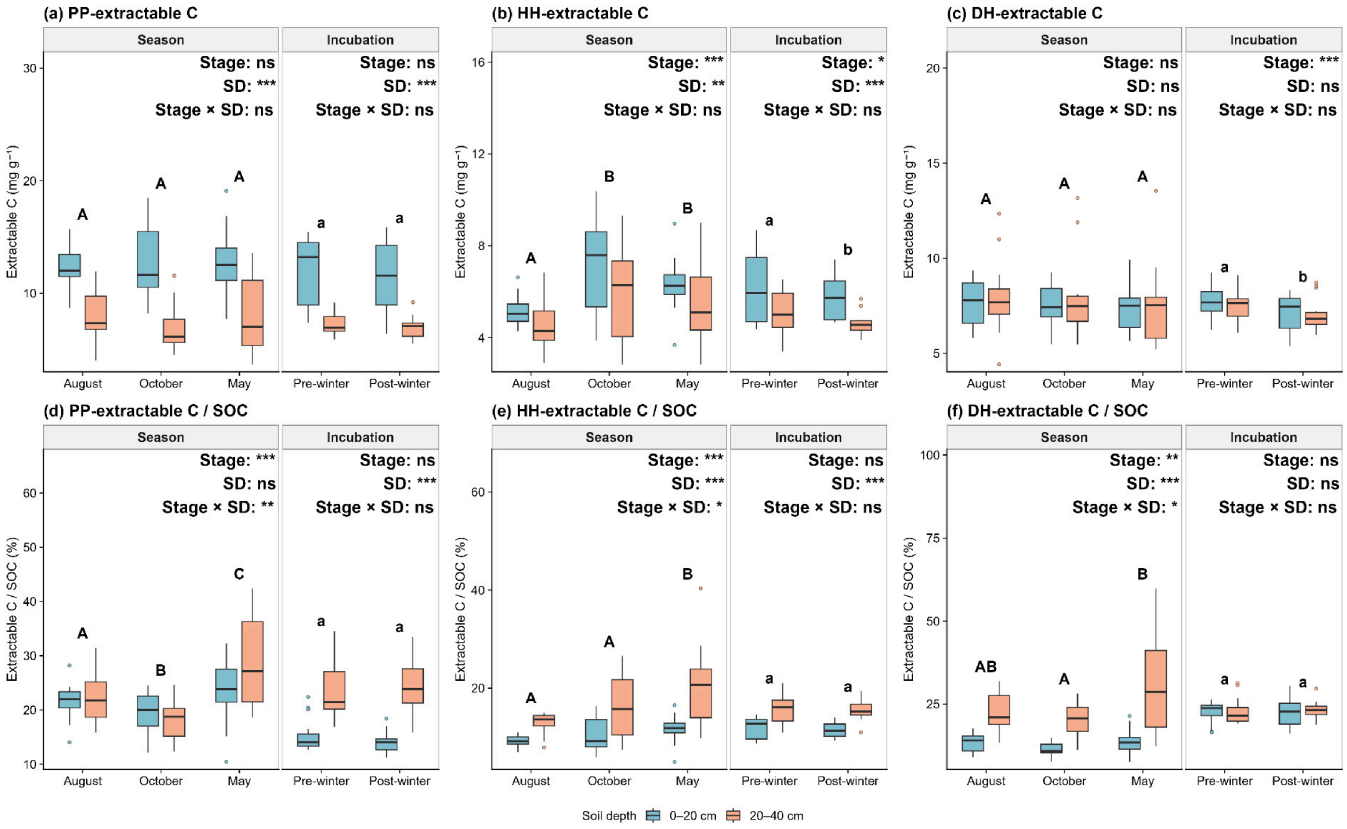


Figure 2. Absolute concentrations of extractable carbon (**a**–**c**) and their proportions relative to soil organic carbon (SOC; **d**–**f**) across seasonal sampling periods (Season) and vegetation-removal incubation stages (Incubation) at different soil depths (SDs). Soil samples were extracted using sodium pyrophosphate (PP), acidified hydroxylamine (HH), and dithionite–HCl (DH). The effects of sampling period or incubation stage (Stage), soil depth (SD), and their interaction (Stage × SD) were assessed using linear mixed-effects models (LMMs). Different uppercase letters indicate significant differences among seasonal sampling periods (marginal means over depth), whereas different lowercase letters indicate significant differences between pre-winter and post-winter incubation stages (marginal means over depth). Significance levels are indicated as ns ($p \geq 0.05$), * ($p < 0.05$), ** ($p < 0.01$), and *** ($p < 0.001$).

Contrary to the extracted metals, the extracted C showed different patterns between the season and vegetation-removal incubation systems. Among the seasonal samples, only C_{HH} differed significantly among sampling periods (Figure 2). The C_{HH} was significantly lower in August than in October and May, increasing by 34.2% from August to October and subsequently decreasing by 9.7% from October to May. The C_{PP} and C_{DH} did not differ significantly among seasons. In contrast, the proportions of the extractable carbon fractions relative to SOC differed significantly among seasons and showed patterns that were not fully consistent with those of the absolute extractable carbon concentrations (Figure 2). The proportions of C_{PP} and C_{DH} to SOC were highest in May, followed by August and October. The proportion of C_{HH} relative to SOC increased in the order August < October < May. C_{PP} and C_{HH} were significantly higher in the 0–20 cm layer than in the 20–40 cm layer, whereas the proportions of C_{HH} and C_{DH} to SOC were significantly lower in the 0–20 cm layer than in the 20–40 cm layer. In addition, a significant interaction effect between season and soil depth was noted in the proportion of C_{PP}, C_{HH}, and C_{DH} to SOC (Figure 2).

The C_{HH} and C_{PP} were significantly positively correlated with SOC, DOC, MBC, and ECEC, but significantly negatively correlated with soil pH in both the seasonal and vegetation- and root-removal incubation datasets. The C_{DH} was significantly positively correlated with DOC in the seasonal system and with SOC and ECEC in the vegetation-

removal incubation system. In addition, C_{DH} was significantly negatively correlated with soil pH in the incubation system (Figure 3).

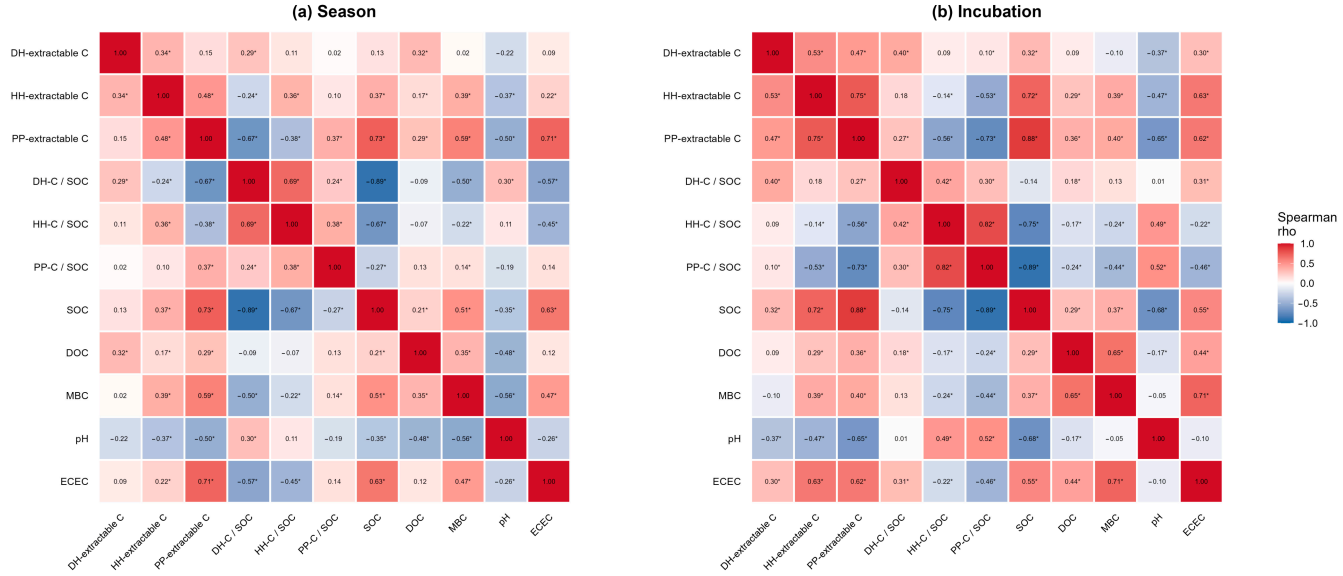


Figure 3. Spearman correlation matrices of extractable carbon fractions and selected soil physicochemical properties across seasonal sampling periods (Season; **a**) and vegetation-removal incubation stages (Incubation; **b**). Extractable carbon fractions were determined using sodium pyrophosphate (PP), acidified hydroxylamine (HH), and dithionite–HCl (DH). C/SOC represents the proportion of extractable carbon relative to soil organic carbon (SOC). DOC, dissolved organic carbon; MBC, microbial biomass carbon; ECEC, effective cation exchange capacity. Correlation analyses were performed separately for Season and Incubation. Cell colors and values represent Spearman's rank correlation coefficients (ρ), ranging from −1 (blue) to +1 (red). Uncertainty was assessed using a Site-stratified, Plot-level cluster bootstrap to account for repeated measurements within plots. Asterisks (*) indicate correlations for which the unadjusted 95% bootstrap confidence intervals exclude zero.

3.4. Variation in the Molar Ratio of Carbon to Metal

We use the molar ratio of C to metal (Al + Fe) to provide an indication of the OMA structure [49]. The molar ratio of C to metals (Al + Fe) (C/M) was calculated to determine the structure of organo-mineral associations in dissolved phases [49]. The C/M varied widely among different extractions in the following ascending order: DH < HH < PP (Figure 4).

In the seasonal system, C/M_{HH} and C/M_{DH} were significantly affected by season and exhibited similar temporal patterns (Figure 4). Both ratios increased from August to October and subsequently decreased from October to May. In contrast, C/M_{PP} did not differ significantly among seasons but varied significantly with soil depth. On average, C/M_{PP} was 25.0% higher in the 0–20 cm layer than in the 20–40 cm layer.

In the vegetation-removal incubation system, both C/M_{PP} and C/M_{DH} were significantly affected by winter-spanning incubation and soil depth (Figure 4). On average, C/M_{PP} and C/M_{DH} decreased by 14.7% and 14.1%, respectively, after winter-spanning incubation. Moreover, C/M_{PP} and C/M_{DH} were 32.8% and 13.5% higher, respectively, in the 0–20 cm layer than in the 20–40 cm layer.

Across both season and vegetation-removal incubation systems, PP, HH, and DH extracted C were significantly positively correlated with the concentrations of co-extracted metals (Al + Fe, Figure 5).

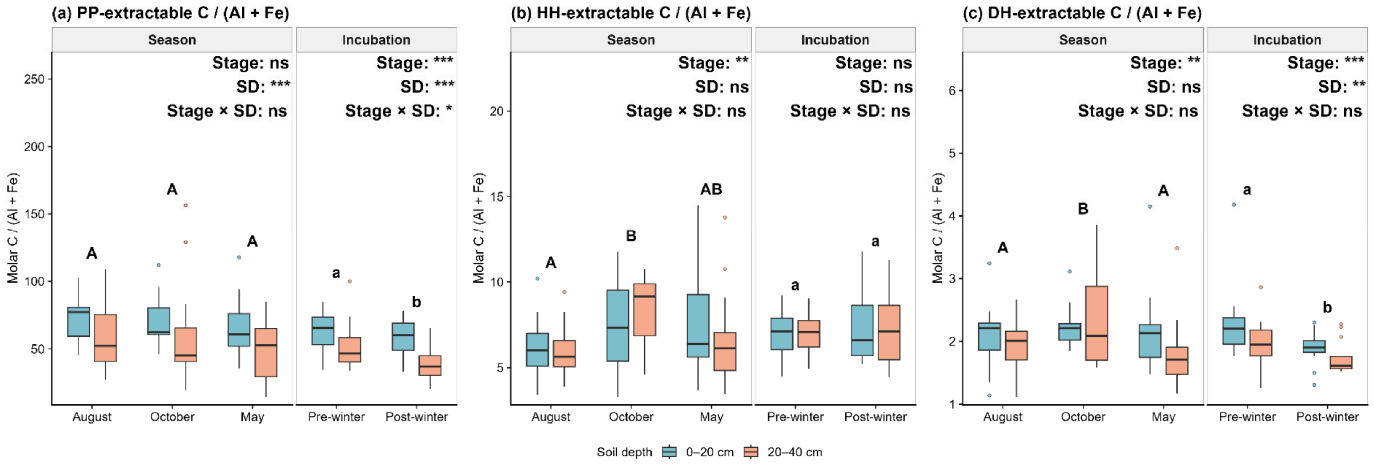


Figure 4. Molar ratios of extractable carbon to metals (Al + Fe) across seasonal sampling periods (Season) and vegetation removal incubation stages (Incubation) at different soil depths (SDs). Soil samples were extracted using sodium pyrophosphate (PP; **a**), acidified hydroxylamine (HH; **b**), and dithionite–HCl (DH; **c**). The effects of sampling period or incubation stage (Stage), soil depth (SD), and their interaction (Stage × SD) were assessed using linear mixed-effects models (LMMs). Different uppercase letters indicate significant differences among seasonal sampling periods (marginal means over depth), whereas different lowercase letters indicate significant differences between pre-winter and post-winter incubation stages (marginal means over depth). Significance levels are indicated as ns ($p \geq 0.05$), * ($p < 0.05$), ** ($p < 0.01$), and *** ($p < 0.001$).

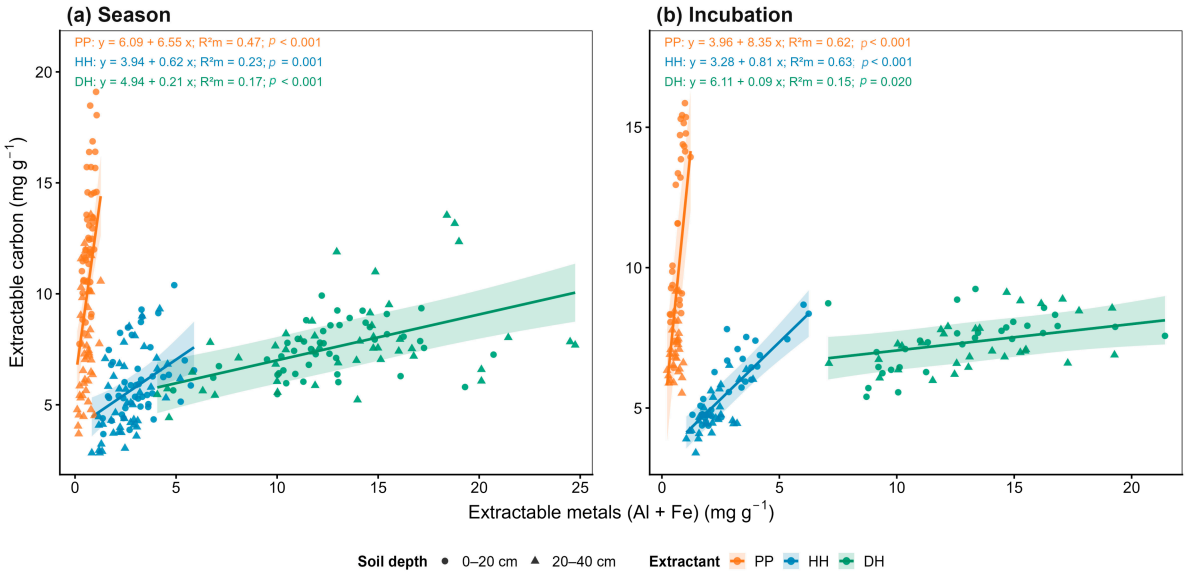


Figure 5. Relationships between extractable carbon and metals (Al + Fe) across seasonal sampling periods (Season; **a**) and vegetation removal incubation stages (Incubation; **b**). Soil samples were extracted using sodium pyrophosphate (PP), acidified hydroxylamine (HH), and dithionite–HCl (DH). The relationships were assessed using linear mixed-effects models, accounting for sampling stage, soil depth, and the hierarchical sampling structure. Solid lines represent model-fitted relationships, and shaded areas indicate 95% confidence intervals. R^2m represents the marginal coefficient of determination of the linear mixed-effects model, and *p*-values indicate the significance of the corresponding metal concentration effects.

4. Discussion

4.1. Spatio-Temporal Variation of Al and Fe Mineral Fractions

From October to May, the Al_{PP} and Fe_{PP} increased in both season and vegetation-removal incubation systems. These increases may be partly associated with the formation of organo-Al and organo-Fe complexes. This interpretation is supported by the increases in DOC and exchangeable Al^{3+} and Fe^{3+} from October to May (Tables 1 and S1), as well as the positive correlations of DOC with C_{PP} (Figure 3), Al^{3+} with Al_{PP}, and Fe^{3+} with Fe_{PP} (Table S1). The effects of winter-spanning processes, such as freeze–thaw cycles, on the release of DOC and exchangeable cations have been widely reported [30,31,37,52]. We therefore hypothesize that winter-spanning may promote organo-metal complex formation by increasing the availability of both organic ligands and metal cations. However, the increases in Al_{PP} and Fe_{PP} were more pronounced at 20–40 cm than at 0–20 cm (Figure 1). This depth pattern may be consistent with the downward redistribution of organo-metal complexes during winter, although it does not directly demonstrate their transport. Similarly, the Al_{HH} and Fe_{HH} in 20–40 cm also increased from October to May but only in the season system (Figure 1). This pattern may indicate that some of the redistributed metals were subsequently associated with non-crystalline phases. Our results are consistent with those of Collignon et al., who found that the effect of depth on oxalate-extractable Al was more pronounced in November and February than in May and August, and suggested that soluble Al progressively migrated through the soil profile during autumn and winter [27]. Nevertheless, changes in extractable metal concentrations may reflect several processes, including changes in solubility, redistribution among extractable pools, and other seasonal processes. Direct evidence for complex formation or transport would require additional measurements, such as mineralogical characterization, pore-water chemistry, or tracer-based transport estimates. Therefore, the proposed formation and redistribution mechanisms should be regarded as hypotheses rather than definitive explanations.

The highest concentrations of Fe_{DH} were found in August and then sharply decreased by 28.4% in October and reached the lowest concentration. This result is again consistent with Collignon et al., who found that levels of dithionite-citrate-bicarbonate extractable Fe were greater in August than in November [27]. The elevated Fe_{DH} concentration in August may be associated with greater Fe availability for Fe-oxide formation, which may, in turn, be related to enhanced mineral weathering during summer [53]. In addition, the Fe_{DH} also decreased by 11.4% from August to pre-winter in the vegetation-removal incubation system (Figure 1). The decline in Fe_{DH} from August to October in both the season system and the vegetation-removal incubation system suggests that changes in Fe oxide pools may be associated with both biotic and abiotic processes. However, the specific mechanisms underlying these changes from summer to autumn require further investigation.

4.2. Effect of Winter-Spanning on Organo-Mineral Associations

The correlation analyses showed different patterns between the pre-winter and post-winter samples. In particular, the association between DOC or MBC and selected extractable C fractions was weaker in the post-winter dataset than in the pre-winter dataset (Table S3). In the vegetation-removal incubation system, the C_{DH} decreased slightly but significantly (by approximately 7.7%) after winter-spanning, whereas no corresponding decrease was observed in the seasonal system. This difference may be related to the increase in soil pH in the vegetation-removal incubation system, in contrast to the relatively stable pH in the season system, given that soil pH was negatively correlated with C_{DH} in the vegetation-removal incubation systems (Figure 3). One possible explanation for this negative correlation is that lower pH protonates hydroxyl groups on Al and Fe oxides, potentially strengthening their interactions with negatively charged soil organic compounds [54]. However, the correlation

does not establish that pH caused the observed change in C_{DH}. Other factors, including temperature, moisture, microbial activity, substrate availability, and soil physical conditions, may also have contributed. The post-winter decrease in C/M_{PP} may also indicate a change in the composition of the operationally defined organo-metal pool. Such a change could potentially affect complex stability, as the stability constants of metal-humic complexes decrease curvilinearly with increasing metal coverage [55,56]. However, this interpretation remains speculative and requires further investigation. Selective-dissolution results indicate changes in an operationally defined extractable pool; they do not, by themselves, demonstrate changes in carbon stability or persistence.

4.3. Seasonal Dynamics of Mineral-Associated C

SOC concentration was higher in October than in August or May. This pattern may reflect the combined effects of new organic matter inputs and reduced microbial activity as temperatures decline, resulting in a net accumulation of SOC. It is broadly consistent with autumn peaks in SOC reported in other studies of seasonal dynamics [57,58]. Other studies have found contrasting or non-significant seasonal patterns, suggesting that SOC responses depend on local environmental conditions and land management [59,60]. Consistent with the SOC pattern, C_{HH} was higher in October than in August. From August to October, C_{HH} increased by 34.2%, while the proportion of C_{HH} to SOC increased 20.9% (Figure 2). C/M_{HH} was also significantly higher in October than in August (Figure 4). These changes may have several explanations. First, some of the additional SOC may have become associated with SRO or other poorly crystalline minerals between August and October. Consistent with this possibility, C/M_{HH} in October in the seasonal system was 15.5% higher than in the pre-winter vegetation removal incubation system. Second, vegetation removal was intended to reduce ongoing root inputs and may have altered the adsorption or desorption of compounds at the mineral water interface, potentially displacing previously adsorbed SOC from mineral surfaces [10,21,61].

C_{HH} also increased by 16.6% from August in the season system to pre-winter in the vegetation-removal incubation system (Figure 2). The SRO mineral-associated C are sensitive to root exudates (especially organic acids) and low-molecular-weight organic molecules released by microorganisms. Keiluweit et al. found that addition of oxalic acid (a common root exudate) could disrupt OMAs and liberate mineral-associated C into pore water, especially in SRO phases [20]. Finley et al. also found that addition of simple and complex C substrates to soils may enhance decomposition of native SOC to a greater degree in soils with a high abundance of SRO mineral phases, indicating the displacement of the native SOC with the new, stronger adsorbing organic compounds [21]. C_{DH} and C_{PP} did not differ significantly among the three seasonal sampling periods. However, seasonal patterns are not uniform among ecosystems, and the present data cannot identify which seasonal driver was responsible for the observed October values. The absence of a significant seasonal difference in C_{DH} and C_{PP} should likewise not be interpreted as evidence that those fractions were intrinsically stable.

The C/SOC proportions and C/(Al + Fe) ratios provide complementary descriptions of the measured extracts. An increase in the proportion of an extractable fraction relative to SOC may result from a change in the numerator, the SOC denominator, or both. It does not by itself demonstrate preferential preservation or slower degradation. Likewise, a change in C/(Al + Fe) indicates a change in the relative amounts of extracted C and metals, but does not directly quantify binding strength or carbon residence time. Overall, the results show that these operationally defined extracts and their ratios vary over short timescales. Further investigation is needed to determine the mechanisms underlying these patterns and their implications for long-term C persistence.

4.4. Limitations

In the vegetation removal incubation, some extractable C measures changed between the pre-winter and post-winter sampling times. However, because the incubation lacked a non-freezing control and the removal treatment may have altered soil structure, organic inputs, and microbial activity, these differences cannot be attributed solely to FT or to the removal of root exudates. The comparison with field samples is informative about contrasting sampling conditions but is not a controlled estimate of the isolated effect of vegetation or root inputs. In addition, the field sampling covered only three periods within a single annual cycle. Therefore, differences among August, October, and May represent site-specific seasonal associations rather than evidence of a recurring long-term pattern. Changes between October and May may reflect multiple concurrent processes, including variations in temperature, soil moisture, plant inputs, microbial activity, and other biogeochemical conditions. Because soil temperature and moisture were not monitored, their contributions to the observed patterns could not be directly evaluated.

5. Conclusions

This study found short-term variation in operationally defined Al- and Fe-associated C fractions across seasonal field samples and between two winter-spanning sampling times in a vegetation removal incubation. C_{HH} was highest in October, whereas C_{PP} and C_{DH} did not differ significantly among seasonal sampling periods. In the incubation, C_{DH} decreased between the pre-winter and post-winter sampling times; however, the lack of a non-freezing control means that this difference cannot be attributed exclusively to FT. The observed C/SOC proportions and C/(Al + Fe) ratios describe changes in the measured extracts but do not directly quantify carbon persistence or stability. Overall, the results demonstrate that extractable fractions and their ratios can vary over short timescales in this alpine forest–shrub transitional zone. Multi-year observations, together with experiments incorporating appropriate non-freezing controls, soil microclimate monitoring, and direct measurements of mineralogy or C turnover, are needed to identify the mechanisms underlying these patterns.

Supplementary Materials: The following supporting information can be downloaded at: https://www.mdpi.com/article/10.3390/f17111381/s1, Table S1: Soil exchangeable cations in different sampling stage; Table S2: Correlation matrix, lower triangle showing Spearman's correlation coefficients between Al and Fe extracted by different extractants in incubation and season systems; Table S3: Correlation matrix, lower triangle showing Spearman's correlation coefficients between extracted C, metal and labile C in different sampling stage.

Author Contributions: M.C. and Y.S. (Yinying Shuai): Visualization, Writing—review and editing, and Software. J.L. and Y.S. (Yuting Song): Software, Methodology, and formal analysis. R.W. and H.Y.: Sample collection and preparation. M.C., M.L. and G.X.: Conceptualization, Methodology, Funding acquisition. All authors have read and agreed to the published version of the manuscript.

Funding: This research was funded by the Natural Science Foundation of Southwest University of Science and Technology (22ZX7113).

Data Availability Statement: Data will be made available upon request.

Conflicts of Interest: The authors declare no conflicts of interest.

References

1. Luo, Z.; Wang, E.; Sun, O.J. Soil Carbon Change and Its Responses to Agricultural Practices in Australian Agro-Ecosystems: A Review and Synthesis. *Geoderma* **2010**, *155*, 211–223. [CrossRef]
2. Maraseni, T.N.; Pandey, S.S. Can Vegetation Types Work as an Indicator of Soil Organic Carbon? An Insight from Native Vegetations in Nepal. *Ecol. Indic.* **2014**, *46*, 315–322. [CrossRef]

3. Schmidt, M.W.I.; Torn, M.S.; Abiven, S.; Dittmar, T.; Guggenberger, G.; Janssens, I.A.; Kleber, M.; Kögel-Knabner, I.; Lehmann, J.; Manning, D.A.C.; et al. Persistence of Soil Organic Matter as an Ecosystem Property. *Nature* **2011**, *478*, 49–56. [CrossRef]
4. Giannetta, B.; Plaza, C.; Vischetti, C.; Cotrufo, M.F.; Zaccone, C. Distribution and Thermal Stability of Physically and Chemically Protected Organic Matter Fractions in Soils across Different Ecosystems. *Biol. Fertil. Soils* **2018**, *54*, 671–681. [CrossRef]
5. Plante, A.F.; Fernández, J.M.; Haddix, M.L.; Steinweg, J.M.; Conant, R.T. Soil Biology & Biochemistry Biological, Chemical and Thermal Indices of Soil Organic Matter Stability in Four Grassland Soils. *Soil Biol. Biochem.* **2011**, *43*, 1051–1058. [CrossRef]
6. Stone, M.M.; Plante, A.F. Relating the Biological Stability of Soil Organic Matter to Energy Availability in Deep Tropical Soil Profiles. *Soil Biol. Biochem.* **2015**, *89*, 162–171. [CrossRef]
7. Mikutta, R.; Kleber, M.; Torn, M.S.; Jahn, R. Stabilization of Soil Organic Matter: Association with Minerals or Chemical Recalcitrance? *Biogeochemistry* **2006**, *77*, 25–56. [CrossRef]
8. Lalonde, K.; Mucci, A.; Ouellet, A.; Gélinas, Y. Preservation of Organic Matter in Sediments Promoted by Iron. *Nature* **2012**, *483*, 198–200. [CrossRef]
9. Hemingway, J.D.; Rothman, D.H.; Grant, K.E.; Rosengard, S.Z.; Eglinton, T.I.; Derry, L.A.; Galy, V.V. Mineral Protection Regulates Long-Term Global Preservation of Natural Organic Carbon. *Nature* **2019**, *570*, 228–231. [CrossRef]
10. Kleber, M.; Eusterhues, K.; Keiluweit, M.; Mikutta, C.; Mikutta, R.; Nico, P.S. *Mineral-Organic Associations: Formation, Properties, and Relevance in Soil Environments*; Elsevier Ltd.: London, UK, 2015; Volume 130.
11. Wagai, R.; Mayer, L.M.; Kitayama, K.; Shirato, Y. Association of Organic Matter with Iron and Aluminum across a Range of Soils Determined via Selective Dissolution Techniques Coupled with Dissolved Nitrogen Analysis. *Biogeochemistry* **2013**, *112*, 95–109. [CrossRef]
12. Chen, C.; Hall, S.J.; Coward, E.; Thompson, A. Iron-Mediated Organic Matter Decomposition in Humid Soils Can Counteract Protection. *Nat. Commun.* **2020**, *11*, 2255. [CrossRef]
13. Hernandez-Soriano, M.C.; Dalal, R.C.; Warren, F.J.; Wang, P.; Green, K.; Tobin, M.J.; Menzies, N.W.; Kopittke, P.M. Soil Organic Carbon Stabilization: Mapping Carbon Speciation from Intact Microaggregates. *Environ. Sci. Technol.* **2018**, *52*, 12275–12284. [CrossRef]
14. Rasmussen, C.; Southard, R.J.; Horwath, W.R. Mineral Control of Organic Carbon Mineralization in a Range of Temperate Conifer Forest Soils. *Glob. Change Biol.* **2006**, *12*, 834–847. [CrossRef]
15. Rasmussen, C.; Southard, R.J.; Horwath, W.R. Litter Type and Soil Minerals Control Temperate Forest Soil Carbon Response to Climate Change. *Glob. Change Biol.* **2008**, *14*, 2064–2080. [CrossRef]
16. Eusterhues, K.; Neidhardt, J.; Hädrich, A.; Küsel, K.; Totsche, K.U. Biodegradation of Ferrihydrite-Associated Organic Matter. *Biogeochemistry* **2014**, *119*, 45–50. [CrossRef]
17. Kögel-Knabner, I.; Guggenberger, G.; Kleber, M.; Kandeler, E.; Kalbitz, K.; Scheu, S.; Eusterhues, K.; Leinweber, P. Organo-Mineral Associations in Temperate Soils: Integrating Biology, Mineralogy, and Organic Matter Chemistry. *J. Plant Nutr. Soil Sci.* **2008**, *171*, 61–82. [CrossRef]
18. Heckman, K.; Lawrence, C.R.; Harden, J.W. A Sequential Selective Dissolution Method to Quantify Storage and Stability of Organic Carbon Associated with Al and Fe Hydroxide Phases. *Geoderma* **2018**, *312*, 24–35. [CrossRef]
19. Che, M.; Gong, Y.; Xu, M.; Kang, C.; Lv, C.; He, S.; Zheng, J. Effects of Elevation and Slope Aspect on the Distribution of the Soil Organic Carbon Associated with Al and Fe Mineral Phases in Alpine Shrub–Meadow Soil. *Sci. Total Environ.* **2021**, *753*, 141933. [CrossRef]
20. Keiluweit, M.; Bougoure, J.J.; Nico, P.S.; Pett-Ridge, J.; Weber, P.K.; Kleber, M. Mineral Protection of Soil Carbon Counteracted by Root Exudates. *Nat. Clim. Change* **2015**, *5*, 588–595. [CrossRef]
21. Finley, B.K.; Dijkstra, P.; Rasmussen, C.; Schwartz, E.; Mau, R.L.; Liu, X.J.A.; van Gestel, N.; Hungate, B.A. Soil Mineral Assemblage and Substrate Quality Effects on Microbial Priming. *Geoderma* **2018**, *322*, 38–47. [CrossRef]
22. Clemmensen, K.E.; Bahr, A.; Ovaskainen, O.; Dahlberg, A.; Ekblad, A.; Wallander, H.; Stenlid, J.; Finlay, R.D.; Wardle, D.A.; Lindahl, B.D. Roots and Associated Fungi Drive Long-Term Carbon Sequestration in Boreal Forest. *Science* **2013**, *339*, 1615–1618. [CrossRef]
23. Yu, G.; Xiao, J.; Hu, S.; Polizzotto, M.L.; Zhao, F.; McGrath, S.P.; Li, H.; Ran, W.; Shen, Q. Mineral Availability as a Key Regulator of Soil Carbon Storage. *Environ. Sci. Technol.* **2017**, *51*, 4960–4969. [CrossRef]
24. Masiello, C.A.; Chadwick, O.A.; Southon, J.; Torn, M.S.; Harden, J.W. Weathering Controls on Mechanisms of Carbon Storage in Grassland Soils. *Glob. Biogeochem. Cycles* **2004**, *18*, GB4023. [CrossRef]
25. Lawrence, C.R.; Harden, J.W.; Xu, X.; Schulz, M.S.; Trumbore, S.E. Long-Term Controls on Soil Organic Carbon with Depth and Time: A Case Study from the Cowlitz River Chronosequence, WA USA. *Geoderma* **2015**, *247–248*, 73–87. [CrossRef]
26. Garcia Arredondo, M.; Lawrence, C.R.; Schulz, M.S.; Tfaily, M.M.; Kukkadapu, R.; Jones, M.E.; Boye, K.; Keiluweit, M. Root-Driven Weathering Impacts on Mineral-Organic Associations in Deep Soils over Pedogenic Time Scales. *Geochim. Cosmochim. Acta* **2019**, *263*, 68–84. [CrossRef]

27. Collignon, C.; Ranger, J.; Turpault, M.P. Seasonal Dynamics of Al- and Fe-Bearing Secondary Minerals in an Acid Forest Soil: Influence of Norway Spruce Roots (*Picea abies* (L.) Karst.). *Eur. J. Soil Sci.* **2012**, *63*, 592–602. [CrossRef]
28. Hall, S.J.; Berhe, A.A.; Thompson, A. Order from Disorder: Do Soil Organic Matter Composition and Turnover Co-Vary with Iron Phase Crystallinity? *Biogeochemistry* **2018**, *140*, 93–110. [CrossRef]
29. Yu, X.; Zou, Y.; Jiang, M.; Lu, X.; Wang, G. Response of Soil Constituents to Freeze-Thaw Cycles in Wetland Soil Solution. *Soil Biol. Biochem.* **2011**, *43*, 1308–1320. [CrossRef]
30. Song, Y.; Zou, Y.; Wang, G.; Yu, X. Altered Soil Carbon and Nitrogen Cycles Due to the Freeze-Thaw Effect: A Meta-Analysis. *Soil Biol. Biochem.* **2017**, *109*, 35–49. [CrossRef]
31. Vestgarden, L.S.; Austnes, K. Effects of Freeze-Thaw on C and N Release from Soils below Different Vegetation in a Montane System: A Laboratory Experiment. *Glob. Change Biol.* **2009**, *15*, 876–887. [CrossRef]
32. Tierney, G.L.; Fahey, T.J.; Groffman, P.M.; Hardy, J.P.; Fitzhugh, R.D.; Driscoll, C.T. Soil Freezing Alters Fine Root Dynamics in a Northern Hardwood Forest. *Biogeochemistry* **2001**, *56*, 175–190. [CrossRef]
33. Risk, N.; Snider, D.; Wagner-Riddle, C. Mechanisms Leading to Enhanced Soil Nitrous Oxide Fluxes Induced by Freeze-Thaw Cycles. *Can. J. Soil Sci.* **2013**, *93*, 401–414. [CrossRef]
34. Oztas, T.; Fayetorbay, F. Effect of Freezing and Thawing Processes on Soil Aggregate Stability. *Catena* **2003**, *52*, 1–8. [CrossRef]
35. Matzner, E.; Borken, W. Do Freeze-Thaw Events Enhance C and N Losses from Soils of Different Ecosystems? A Review. *Eur. J. Soil Sci.* **2008**, *59*, 274–284. [CrossRef]
36. Zhang, Z.; Ma, W.; Feng, W.; Xiao, D.; Hou, X. Reconstruction of Soil Particle Composition During Freeze-Thaw Cycling: A Review. *Pedosphere* **2016**, *26*, 167–179. [CrossRef]
37. Du, L.; Dyck, M.; Shotyk, W.; He, H.; Lv, J.; Cuss, C.W.; Bie, J. Lead Immobilization Processes in Soils Subjected to Freeze-Thaw Cycles. *Ecotoxicol. Environ. Saf.* **2020**, *192*, 110288. [CrossRef]
38. Liu, Q.; Wu, Y.; Hu, J.; Chen, D.; Zhao, W.; Tan, H.; Liu, Q. Distinct Patterns of Soil Bacterial and Fungal Communities in the Alpine Treeline and Shrubline Ecotone on the Eastern Tibetan Plateau. *Forests* **2026**, *17*, 510. [CrossRef]
39. Sigdel, S.R.; Zheng, X.; Babst, F.; Camarero, J.J.; Gao, S.; Li, X.; Lu, X.; Pandey, J.; Dawadi, B.; Sun, J.; et al. Accelerated Succession in Himalayan Alpine Treelines under Climatic Warming. *Nat. Plants* **2024**, *10*, 1909–1918. [CrossRef]
40. Lu, X.; Zheng, X.; Liang, E.; Piao, S.; Babst, F.; Elliott, G.P.; Sigdel, S.R.; Wang, T.; Wang, Y.; Li, X.; et al. Patterns, Dynamics and Drivers of Alpine Treelines and Shrublines. *Nat. Rev. Earth Environ.* **2025**, *6*, 489–502. [CrossRef]
41. Wang, C.; Liu, R.; Zhang, D.; Chen, B.; Peng, B.; Yang, Y. Bacterial and Fungal Community Shifts Across an Alpine Forest–Grassland Ecotone in the Yili River Valley, Xinjiang. *Forests* **2026**, *17*, 1177. [CrossRef]
42. Chen, L.F.; He, Z.B.; Du, J.; Yang, J.J.; Zhu, X. Patterns and Environmental Controls of Soil Organic Carbon and Total Nitrogen in Alpine Ecosystems of Northwestern China. *Catena* **2016**, *137*, 37–43. [CrossRef]
43. Hoffmann, U.; Hoffmann, T.; Johnson, E.A.; Kuhn, N.J. Assessment of Variability and Uncertainty of Soil Organic Carbon in a Mountainous Boreal Forest (Canadian Rocky Mountains, Alberta). *Catena* **2014**, *113*, 107–121. [CrossRef]
44. Zhu, W.Z.; Xiang, J.S.; Wang, S.G.; Li, M.H. Resprouting Ability and Mobile Carbohydrate Reserves in an Oak Shrubland Decline with Increasing Elevation on the Eastern Edge of the Qinghai-Tibet Plateau. *For. Ecol. Manag.* **2012**, *278*, 118–126. [CrossRef]
45. Kaiser, K.; Guggenberger, G.; Haumaier, L.; Zech, W. The Composition of Dissolved Organic Matter in Forest Soil Solutions: Changes Induced by Seasons and Passage through the Mineral Soil. *Org. Geochem.* **2002**, *33*, 307–318. [CrossRef]
46. Hansen, M.; Bang-Andreasen, T.; Sørensen, H.; Ingerslev, M. Micro Vertical Changes in Soil pH and Base Cations over Time after Application of Wood Ash on Forest Soil. *For. Ecol. Manag.* **2017**, *406*, 274–280. [CrossRef]
47. Shi, L.; Zhang, H.; Liu, T.; Mao, P.; Zhang, W.; Shao, Y.; Fu, S. An Increase in Precipitation Exacerbates Negative Effects of Nitrogen Deposition on Soil Cations and Soil Microbial Communities in a Temperate Forest. *Environ. Pollut.* **2018**, *235*, 293–301. [CrossRef]
48. Vance, E.D.; Brggkes, P.C.; Jenkinson, D.S. An Extraction Method for Measuring Soil Microbial Biomass C. *Soil Biol. Biochem.* **1987**, *19*, 703–707. [CrossRef]
49. Coward, E.K.; Thompson, A.T.; Plante, A.F. Iron-Mediated Mineralogical Control of Organic Matter Accumulation in Tropical Soils. *Geoderma* **2017**, *306*, 206–216. [CrossRef]
50. Wagai, R.; Kajiura, M.; Asano, M. Iron and Aluminum Association with Microbially Processed Organic Matter via Meso-Density Aggregate Formation across Soils: Organo-Metallic Glue Hypothesis. *Soil* **2020**, *6*, 597–627. [CrossRef]
51. Porras, R.C.; Hicks Pries, C.E.; McFarlane, K.J.; Hanson, P.J.; Torn, M.S. Association with Pedogenic Iron and Aluminum: Effects on Soil Organic Carbon Storage and Stability in Four Temperate Forest Soils. *Biogeochemistry* **2017**, *133*, 333–345. [CrossRef]
52. Zhang, H.; Tang, J.; Liang, S.; Li, Z.; Wang, J.; Wang, S. Early Thawing after Snow Removal and No Straw Mulching Accelerates Organic Carbon Cycling in a Paddy Soil in Northeast China. *J. Environ. Manag.* **2018**, *209*, 336–345. [CrossRef]
53. Turpault, M.P.; Gobran, G.R.; Bonnaud, P. Temporal Variations of Rhizosphere and Bulk Soil Chemistry in a Douglas Fir Stand. *Geoderma* **2007**, *137*, 490–496. [CrossRef]
54. Berhe, A.A.; Kleber, M. Erosion, Deposition, and the Persistence of Soil Organic Matter: Mechanistic Considerations and Problems with Terminology. *Earth Surf. Process. Landf.* **2013**, *38*, 908–912. [CrossRef]

55. Stevenson, F.J.; Chen, Y. Stability Constants of Copper(II)-Humate Complexes Determined by Modified Potentiometric Titration. *Soil Sci. Soc. Am. J.* **1991**, *55*. [CrossRef]
56. Takahashi, T.; Dahlgren, R.A. Nature, Properties and Function of Aluminum-Humus Complexes in Volcanic Soils. *Geoderma* **2016**, *263*, 110–121. [CrossRef]
57. Wang, X.; Li, J.; Li, L.; Guo, Y.; Guo, B.; Zhao, C. Spatiotemporal Variations in Soil Organic Carbon and Microbial Drivers in the Yellow River Delta Wetland, China. *Sustainability* **2025**, *17*, 5188. [CrossRef]
58. Kravchenko, Y.; Yarosh, A.; Chen, Y. Profile Soil Carbon and Nitrogen Dynamics in Typical Chernozem under Long-Term Tillage Use. *Land* **2022**, *11*, 1165. [CrossRef]
59. Karthik, V.; Vijay Bhaskar, B.; Ramachandran, S.; Zhuang, Q. Dynamics of Organic and Black Carbon in High-Altitude Soils: Insights from Morphological, Chemometric, and Environmental Analyses. *Environ. Pollut.* **2025**, *382*. [CrossRef]
60. Li, N.; Wang, Y.; Li, S.; Xu, T.; Wei, L.; Xu, S.; Zhao, N. Seasonal Plant-Microbial Coupling Regulates Carbon Transformation Pathways and Soil Organic Carbon Persistence in Alpine Grasslands. *Catena* **2026**, *274*, 110528. [CrossRef]
61. Kaiser, K.; Kalbitz, K. Cycling Downwards-Dissolved Organic Matter in Soils. *Soil Biol. Biochem.* **2012**, *52*, 29–32. [CrossRef]

Disclaimer/Publisher's Note: The statements, opinions and data contained in all publications are solely those of the individual author(s) and contributor(s) and not of MDPI and/or the editor(s). MDPI and/or the editor(s) disclaim responsibility for any injury to people or property resulting from any ideas, methods, instructions or products referred to in the content.